Engineering with Computers (2019) 35:593–604
https://doi.org/10.1007/s00366-018-0618-2

ORIGINAL ARTICLE

Analysis and optimal design of scissor-link foldable structures

A. Kaveh[1] · **M. Abedi**[1]

Received: 21 November 2017 / Accepted: 11 May 2018 / Published online: 22 May 2018

Abstract
This paper presents a finite element method for the analysis of scissor-link foldable structures. These structures are capable of deforming from compact form to expanded form, and vice versa. Due to their complex mechanism, it is difficult and time-consuming to simulate foldable structures in analysis softwares, while the proposed method of this paper makes it easy to perform the analysis in a simple manner. In addition, this paper uses two different multi-objective meta-heuristic algorithms, NSGAII and MOCBO, to perform optimum design of foldable structures. The purpose is to find designs that result in minimum weight and minimum volume of the structures satisfying all the constraints consisting of maximum stress, elements buckling, and permissible displacement.

Keywords Scissor-link foldable structures · Finite elements analysis · Optimal design · Meta-heuristic algorithms

1 Introduction

Foldable and deployable structures are accounted in space structures having deformation ability. One category of these structures is scissor-link foldable structures, which contain pined elements acting like scissor mechanism. This mechanism gives the structure the ability to deform from a compact form to an expanded one (Fig. 1).

These structures in folded position occupy less volume, but after expansion cover significant area and can be used as shelters in many places and situations, such as in disasters, wars, contemporary showplaces, and so on. The supports of these structures generally are rollers. This makes it easy for these structures to deform from a folded state to an expanded one. After expanding the structures, the supports can be fixed to the ground by some bars. Also, the structures can be fixed by attaching some cables between the joints.

The scissor mechanism has complicated conditions in the analysis and design of these structures. The goal of this paper is to present a new practical method to facilitate the analysis process of the scissor-link foldable structures.

Analysis of foldable structures has a long history. The primary work [2] presented a compact stiffness matrix for scissor elements in an idealized situation. That stiffness matrix was developed [3] for each pair of scissor elements. The mentioned methods are applicable to a kind of foldable structure with bar elements such that its joints do not transfer any bending moments between its elements. However, the analysis method of this paper is designed for scissor-link foldable structures with the joints being able to transfer bending moments except in the hinged direction to simulate the real scissor mechanism in the structure.

Many papers have been published on the design of these structures. Foldable structures have various shapes; generally, they are divided into three categories: flat, barrel vault, and spherical shape. The design of these structures requires some conditions [4] that provide complete folding ability for the structures. The design of barrel vault foldable structures was studied in Mira et al. [1], Hernandez et al. [5] and Escrig and Valcarcel [6], and various spherical shapes were investigated in Escrig et al. [7] and Escrig and Sanchez [8].

Foldable structures can be expanded in place. After finishing work, they can be folded and be transported to another place and be used again. Due to this advantage, it is beneficial to design lightweight foldable structures to make them easy to be transported. This paper intends to design structures that are lightweight and occupy less space when they are in a folded status, using meta-heuristic optimization algorithms.

✉ A. Kaveh
alikaveh@iust.ac.ir

M. Abedi
meysamabedi19937@gmail.com

[1] Centre of Excellence for Fundamental Studies in Structural Engineering, School of Civil Engineering, Iran University of Science and Technology, Narmak, Tehran-16, Iran

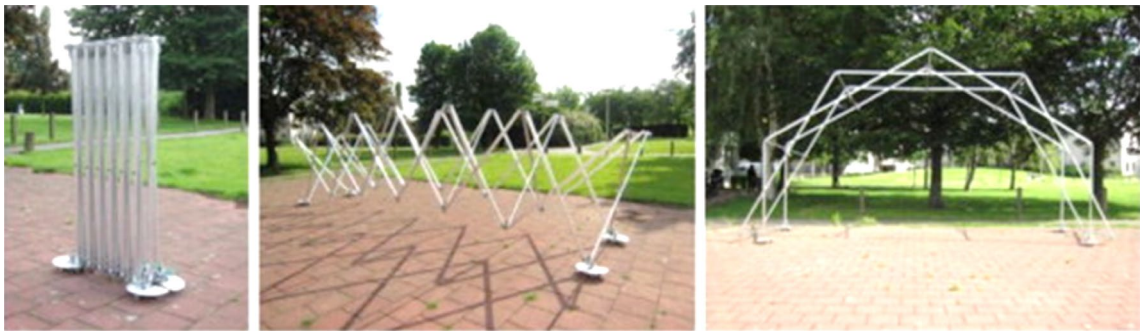

Fig. 1 Folding process of a barrel vault scissor-link foldable structure [1]

Nowadays, meta-heuristic algorithms are considered as powerful tools in various fields to perform optimization. There are many different optimization algorithms named by their origin [9–11]. Recently, scientists have been extending these algorithms to multi-objective ones having the ability to minimize more than one objective function. In structural optimization, these algorithms are used to perform design process automatically by changing the topology of the structure or cross sections of elements.

There are diverse works on optimization of foldable structures. The primary work [12] tried to attain element' cross sections resulting in minimum weight of structures by using the recursive quadratic programming method; also [13, 14] optimization by genetic and ACO algorithms was performed. As recent works [15, 16] used various algorithms to get an optimum shape and elements' sections to reduce the weight of structures, Refs. [17, 18] utilized a multi-objective optimization algorithm, NSGAII, to find the optimum weight and volume for the foldable structures. This paper uses two different algorithms to get an optimum design of foldable structures that result in minimum weight and volume of structure: the first algorithm is NSGAII [19] and the second is multi-objective of colliding bodies optimization [9], provided in Panda and Pani [20].

The rest of this paper is organized as follows. In Sect. 2, a description of the method for analysis of foldable structures is presented. In Sect. 3, the method for design of foldable structures is provided. Then Sect. 4 explains the optimization algorithms for the design. In Sect. 5, numerical examples for optimal design of foldable structures are presented. Finally, concluding remarks are provided in Sect. 6.

2 Analysis of foldable structures

Finite element is a powerful method for structural analysis based on Eq. (1). This equation shows that the displacement (d) of an elastic element is proportional to the applied forces (P) through the stiffness (K):

$$P = K \cdot d. \tag{1}$$

The aim of this paper is to apply the finite element method for the analysis of scissor-link foldable structures. For this purpose, each element is considered as a beam with three nodes pinned in the Z direction to make a scissor mechanism (Fig. 2). Based on the definition of stiffness, the stiffness matrix of the elements is presented in Fig. 3. In this matrix, nodal moments in Z direction do not have stiffness relation with other degrees of freedom of the element because there is hinge in that direction, so that their rows and columns in the stiffness matrix are zero. However, these zero rows and columns make the stiffness matrix singular; this means the structure will not be geometrically stable. In the present method due to restricted hinges, the stiffness matrix becomes geometrically stable. A small number ε is added to the stiffness matrix to constrain the hinges and prevent them from having free behavior. The ε makes the stiffness relation between the nodal moments in the Z direction with themselves. Its value does not have a significant effect on the results of the analysis. In this paper, the magnitude of ε is considered as 0.001.

Other variables are determined by the properties of the element and the material. In foldable structures, elements may have a local axis and local rotation that should be considered in transforming the stiffness matrix into a global coordinate before assembling (2). In the equation, (T) is the transformational matrix and (R) is the rotational matrix. In the scissor-link structures the hinge direction (local Z direction) of the elements varies for different units and this requires considering different element rotational matrixes:

$$K = T'R'kRT. \tag{2}$$

In finite element analysis, the body forces of elements should be equalized in nodal degrees of freedom. Importing gravity force on scissor elements with three nodes is rather complicated, and it depends on the local rotation (θ) of elements (Fig. 2). When gravity load is imposed on the elements in the Z direction ($\theta = \pi/2$), elements act like a two span beams and contain both nodal forces and moments (Eq. 3):

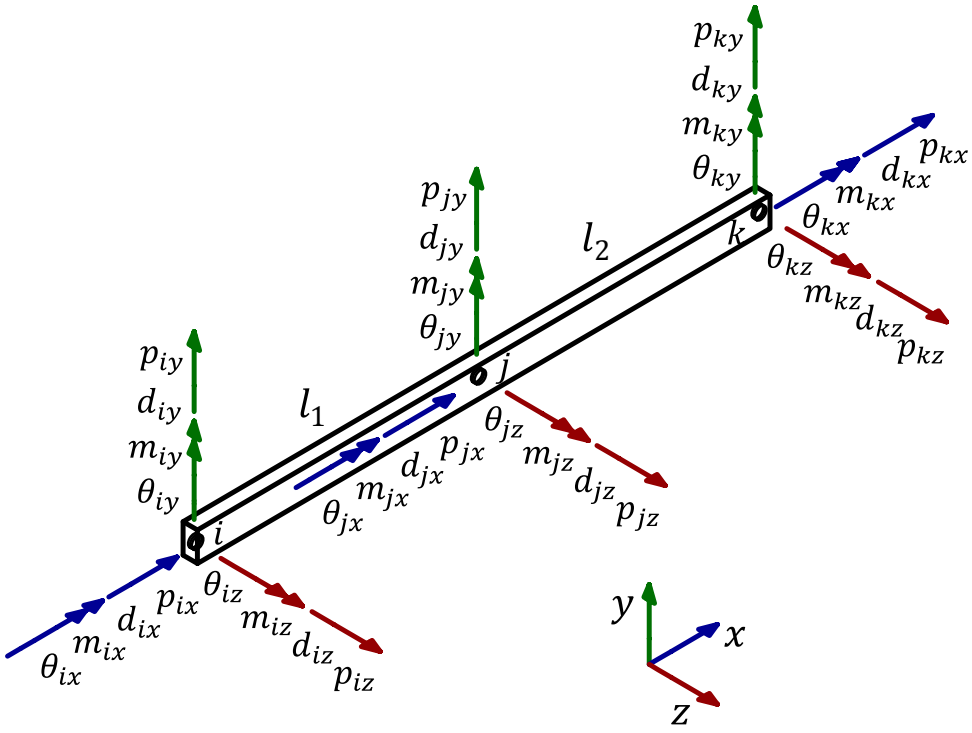

Fig. 2 A three-node scissor element

$$G_1 = [0, p_2, 0, p_4, 0, p_6, 0, p_8 0, p_{10}, 0, p_{12}, 0, p_{14}, 0, p_{16}, 0, p_{18}]', \quad (3)$$

$$p_2 = -(A \times \rho \times l_1/2),$$

$$p_4 = ((A \times \rho \times {l_1}^2/12) \times z_{ki}/L),$$

$$p_6 = -((A \times \rho \times {l_1}^2/12) \times x_{ki}/L),$$

$$p_8 = -(A \times \rho \times L/2),$$

$$p_{10} = ((A \times \rho \times ({l_2}^2 - {l_1}^2)/12) \times z_{ki}/L),$$

$$p_{12} = ((A \times \rho \times ({l_1}^2 - {l_2}^2)/12) \times x_{ki}/L),$$

$$p_{14} = -(A \times \rho \times l_2/2),$$

$$p_{16} = -((A \times \rho \times {l_2}^2/12) \times z_{ki}/L),$$

$$p_{18} = ((A \times \rho \times {l_2}^2/12) \times x_{ki}/L),$$

$$L = l_1 + l_2 \quad z_{ki} = z_k - z_i \quad x_{ki} = x_k - x_i.$$

When the gravity load is imposed in the Y direction ($\theta = 0$), there is no equalized moment in nodes since the elements are hinged in the Z direction. By solving an indeterminate beam with three hinged support the related formulation for this direction, the following formulas are obtained (Eq. 4):

$$G_2 = [0, p_2, 0, 0, 0, 0, 0, p_8, 0, 0, 0, 0, 0, p_{14}, 0, 0, 0, 0]', \quad (4)$$

$$p_2 = -w,$$

$$p_8 = -(A \times \rho \times L^2/(2 \times l_2) - w \times L/l_2),$$

$$p_{14} = -(3 \times A \times \rho \times ({l_1}^3 + {l_2}^3)/(8 \times {l_2}^2) - w \times {l_1}^2/{l_2}^2),$$

$$w = A \times \rho \times (L - L^2/(2 \times l_2) - 3 \times ({l_1}^3 + {l_2}^3)/(8 \times {l_2}^2))/(1 - L/l_2 - (l_1/l_2)^2).$$

Generally for all amounts of θ, nodal forces and moments are obtained by Eq. (5). All forces and moments obtained by the equations are in the global coordinate system. In the equations, A is the area of element section, ρ is the mass density of materials, l_1 and l_2 are lengths of elements (Fig. 2), and x and z are coordinates of the element nodes:

$$G_{\text{total}} = G_1 \times \sin(\theta) + G_2 \times \cos(\theta). \quad (5)$$

3 Design of foldable structures

In all scissor-link foldable structures, Eq. (6) should be satisfied; it is a fundamental condition that gives the structure complete folding ability (Fig. 4). Barrel vault and spherical dome foldable structures are divided into various groups [6]; each of them have their own geometric formulations. In this paper, two-way barrel vault and a kind of spherical dome that previously had been investigated in [8] are presented. For two-way barrel vault of Fig. 5, nodal coordinates are attained by Eq. (7), and for a

$$E\times\begin{bmatrix}
\frac{A}{l_1} & 0 & 0 & 0 & 0 & 0 & -\frac{A}{l_1} & 0 & 0 & 0 & 0 & 0 & 0 & 0 & 0 & 0 & 0 & 0\\
0 & \frac{3\times I_z}{{l_1}^2(l_1+l_2)} & 0 & 0 & 0 & 0 & 0 & -\frac{3\times I_z}{{l_1}^2(l_2)} & 0 & 0 & 0 & 0 & 0 & \frac{3\times I_z}{l_1 l_2(l_1+l_2)} & 0 & 0 & 0 & 0\\
0 & 0 & \frac{12\times I_y}{{l_1}^3} & 0 & -\frac{6\times I_y}{{l_1}^2} & 0 & 0 & 0 & -\frac{12\times I_y}{{l_1}^3} & 0 & -\frac{6\times I_y}{{l_1}^2} & 0 & 0 & 0 & 0 & 0 & 0 & 0\\
0 & 0 & 0 & \frac{J}{2\times l_1(1+\upsilon)} & 0 & 0 & 0 & 0 & 0 & -\frac{J}{2\times l_1(1+\upsilon)} & 0 & 0 & 0 & 0 & 0 & 0 & 0 & 0\\
0 & 0 & -\frac{6\times I_y}{{l_1}^2} & 0 & \frac{4\times I_y}{l_1} & 0 & 0 & 0 & \frac{6\times I_y}{{l_1}^2} & 0 & \frac{2\times I_y}{l_1} & 0 & 0 & 0 & 0 & 0 & 0 & 0\\
0 & 0 & 0 & 0 & 0 & \varepsilon & 0 & 0 & 0 & 0 & 0 & 0 & 0 & 0 & 0 & 0 & 0 & 0\\
-\frac{A}{l_1} & 0 & 0 & 0 & 0 & 0 & \frac{A}{l_1}+\frac{A}{l_2} & 0 & 0 & 0 & 0 & 0 & -\frac{A}{l_2} & 0 & 0 & 0 & 0 & 0\\
0 & -\frac{3\times I_z}{{l_1}^2(l_2)} & 0 & 0 & 0 & 0 & 0 & \frac{3\times I_z(l_1+l_2)}{{l_1}^2{l_2}^2} & 0 & 0 & 0 & 0 & 0 & -\frac{3\times I_z}{{l_2}^2(l_1)} & 0 & 0 & 0 & 0\\
0 & 0 & -\frac{12\times I_y}{{l_1}^3} & 0 & \frac{6\times I_y}{{l_1}^2} & 0 & 0 & 0 & \frac{12\times I_y}{{l_1}^3}+\frac{12\times I_y}{{l_2}^3} & 0 & \frac{6\times I_y}{{l_1}^2}-\frac{6\times I_y}{{l_2}^2} & 0 & 0 & 0 & -\frac{12\times I_y}{{l_2}^3} & 0 & -\frac{6\times I_y}{{l_2}^2} & 0\\
0 & 0 & 0 & -\frac{J}{2\times l_1(1+\upsilon)} & 0 & 0 & 0 & 0 & 0 & \frac{J}{2\times l_1(1+\upsilon)}+\frac{J}{2\times l_2(1+\upsilon)} & 0 & 0 & 0 & 0 & -\frac{J}{2\times l_2(1+\upsilon)} & 0 & 0\\
0 & 0 & -\frac{6\times I_y}{{l_1}^2} & 0 & \frac{2\times I_y}{l_1} & 0 & 0 & 0 & \frac{6\times I_y}{{l_1}^2}-\frac{6\times I_y}{{l_2}^2} & 0 & \frac{4\times I_y}{l_1}+\frac{4\times I_y}{l_2} & 0 & 0 & 0 & \frac{6\times I_y}{{l_2}^2} & 0 & \frac{2\times I_y}{l_2} & 0\\
0 & 0 & 0 & 0 & 0 & 0 & 0 & 0 & 0 & 0 & 0 & \varepsilon & 0 & 0 & 0 & 0 & 0 & 0\\
0 & 0 & 0 & 0 & 0 & 0 & -\frac{A}{l_2} & 0 & 0 & 0 & 0 & 0 & \frac{A}{l_2} & 0 & 0 & 0 & 0 & 0\\
0 & \frac{3\times I_z}{l_1 l_2(l_1+l_2)} & 0 & 0 & 0 & 0 & 0 & -\frac{3\times I_z}{{l_2}^2(l_1)} & 0 & 0 & 0 & 0 & 0 & \frac{3\times I_z}{{l_2}^2(l_1+l_2)} & 0 & 0 & 0 & 0\\
0 & 0 & 0 & 0 & 0 & 0 & 0 & 0 & -\frac{12\times I_y}{{l_2}^3} & 0 & \frac{6\times I_y}{{l_2}^2} & 0 & 0 & 0 & \frac{12\times I_y}{{l_2}^3} & 0 & \frac{6\times I_y}{{l_2}^2} & 0\\
0 & 0 & 0 & 0 & 0 & 0 & 0 & 0 & 0 & -\frac{J}{2\times l_2(1+\upsilon)} & 0 & 0 & 0 & 0 & 0 & \frac{J}{2\times l_2(1+\upsilon)} & 0 & 0\\
0 & 0 & 0 & 0 & 0 & 0 & 0 & 0 & -\frac{6\times I_y}{{l_2}^2} & 0 & \frac{2\times I_y}{l_2} & 0 & 0 & 0 & \frac{6\times I_y}{{l_2}^2} & 0 & \frac{4\times I_y}{l_2} & 0\\
0 & 0 & 0 & 0 & 0 & 0 & 0 & 0 & 0 & 0 & 0 & 0 & 0 & 0 & 0 & 0 & 0 & \varepsilon
\end{bmatrix}$$

$$\begin{bmatrix}
k_{1.1} & & & & & & & & & & & & & & & & & \\
0 & k_{2.2} & & & & & & & & & & & & & & & & \\
0 & 0 & k_{3.3} & & & & & & & & & & & & & & & \\
0 & 0 & 0 & k_{4.4} & & & & & & & & & & & & & & \\
0 & 0 & k_{5.3} & 0 & k_{5.5} & & & & & & & & & & & & & \\
0 & 0 & 0 & 0 & 0 & k_{6.6} & & & & & & & & & & & & \\
k_{7.1} & 0 & 0 & 0 & 0 & 0 & k_{7.7} & & & & & & & & & & & \\
0 & k_{8.2} & 0 & 0 & 0 & 0 & 0 & k_{8.8} & & & & & & & & & & \\
0 & 0 & k_{8.3} & 0 & k_{9.5} & 0 & 0 & 0 & k_{9.9} & & & & & & & & & \\
0 & 0 & 0 & k_{10.4} & 0 & 0 & 0 & 0 & 0 & k_{10.10} & & & & & & & & \\
0 & 0 & k_{10.3} & 0 & k_{11.5} & 0 & 0 & 0 & k_{11.9} & 0 & k_{11.11} & & & & & & & \\
0 & 0 & 0 & 0 & 0 & 0 & 0 & 0 & 0 & 0 & 0 & k_{12.12} & & & & & & \\
0 & 0 & 0 & 0 & 0 & 0 & k_{13.7} & 0 & 0 & 0 & 0 & 0 & k_{13.13} & & & & & \\
0 & k_{14.2} & 0 & 0 & 0 & 0 & 0 & k_{14.8} & 0 & 0 & 0 & 0 & 0 & k_{14.14} & & & & \\
0 & 0 & 0 & 0 & 0 & 0 & 0 & 0 & k_{15.9} & 0 & k_{15.11} & 0 & 0 & 0 & k_{15.15} & & & \\
0 & 0 & 0 & 0 & 0 & 0 & 0 & 0 & 0 & k_{16.10} & 0 & 0 & 0 & 0 & 0 & k_{16.16} & & \\
0 & 0 & 0 & 0 & 0 & 0 & 0 & 0 & k_{17.9} & 0 & k_{17.11} & 0 & 0 & 0 & k_{17.15} & 0 & k_{17.17} & \\
0 & 0 & 0 & 0 & 0 & 0 & 0 & 0 & 0 & 0 & 0 & 0 & 0 & 0 & 0 & 0 & 0 & k_{18.18}
\end{bmatrix}$$

symmetric

$k_{1.1} = -k_{7.1} = E \times A/l_1$

$k_{2.2} = E \times 3 \times I_z/({l_1}^2 \times (l_1 + l_2))$

$k_{8.2} = -E \times 3 \times I_z/({l_1}^2 \times l_2)$

$k_{14.2} = E \times 3 \times I_z/(l_1 \times l_2 \times (l_1 + l_2))$

$k_{3.3} = -k_{8.3} = E \times 12 \times {I_y}/{l_1}^3$

$k_{5.3} = k_{10.3} = -E \times 6 \times {I_y}/{l_1}^2$

$k_{4.4} = -k_{10.4} = E \times J/(2 \times l_1 \times (1 + \upsilon))$

$k_{5.5} = E \times 4 \times I_y/l_1$

$k_{9.5} = E \times 6 \times {I_y}/{l_1}^2$

$k_{11.5} = E \times 2 \times I_y/l_1$

$k_{6.6} = k_{12.12} = k_{18.18} = \varepsilon$

$k_{13.13} = -k_{13.7} = E \times A/l_2$

$k_{7.7} = k_{1.1} + k_{13.13}$

$k_{14.14} = E \times 3 \times I_z/({l_2}^2 \times (l_1 + l_2))$

$k_{15.15} = -k_{15.9} = E \times 12 \times {I_y}/{l_2}^3$

$k_{17.15} = k_{15.11} = E \times 6 \times {I_y}/{l_2}^2$

$k_{16.16} = -k_{16.10} = E \times J/(2 \times l_2 \times (1 + \upsilon))$

$k_{14.8} = -E \times 3 \times I_z/({l_2}^2 \times l_1)$

$k_{17.17} = E \times 4 \times I_y/l_2$

$k_{17.11} = E \times 2 \times I_y/l_2$

$k_{17.9} = -E \times 6 \times {I_y}/{l_2}^2$

$k_{10.10} = k_{4.4} + k_{16.16}$

$k_{11.11} = k_{5.5} + k_{17.17}$

$k_{9.9} = k_{3.3} + k_{15.15}$

$k_{11.9} = k_{9.5} + k_{17.9}$

$k_{8.8} = 3 \times I_z \times (l_1 + l_2)/{l_1}^2 \times {l_2}^2$

Fig. 3 Stiffness matrix of scissor elements

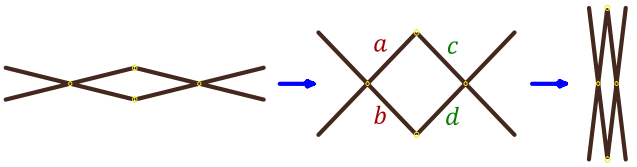

Fig. 4 A scissor mechanism

$$\begin{cases} \alpha_i = 180/(2 \times \text{number of units}) & i = 1 \\ R \times \cos(\alpha_1 + \alpha_i) \times \sin(\alpha_1) = R \times \sin(\alpha_i) & i = 2 \\ R \times \cos\left(\alpha_1 + 2 \times \sum_{j=2}^{i-1} \alpha_j + \alpha_i\right) \times \sin(\alpha_1) = R \times \sin(\alpha_i) & i \geqslant 3 \end{cases} . \tag{8}$$

spherical dome of Fig. 6, Eq. (8) is used. In the presented equations, R, t, and the number of units are determined. The number of units in one arch for the barrel vault and in the base semicircle for spherical dome are considered:

$$a + b = c + d, \tag{6}$$

$$\alpha = 180/\text{number of units}, \quad \sin(s)/(R - t) = \sin(p)/R = \sin(\alpha)/L, \tag{7}$$

4 Optimization of foldable structures

Recently, meta-heuristic algorithms are extensively used in different fields of engineering as a powerful computational tool to find optimum solution of the functions. These algorithms test iteratively sets of variables which result in less cost, while satisfying the constraints. Generally, meta-heuristic algorithms are inspired by natural events. For example, CBO algorithm [9] is inspired from the collision of bodies or VPS algorithm [10] is established on the system of vibrating particles. Figure 7 shows the flowchart of these algorithms:

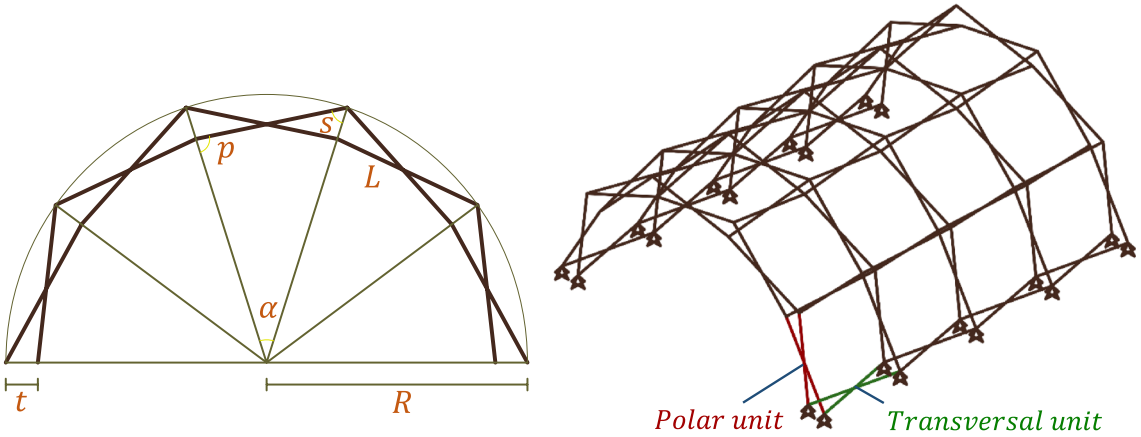

Fig. 5 A barrel vault foldable structure

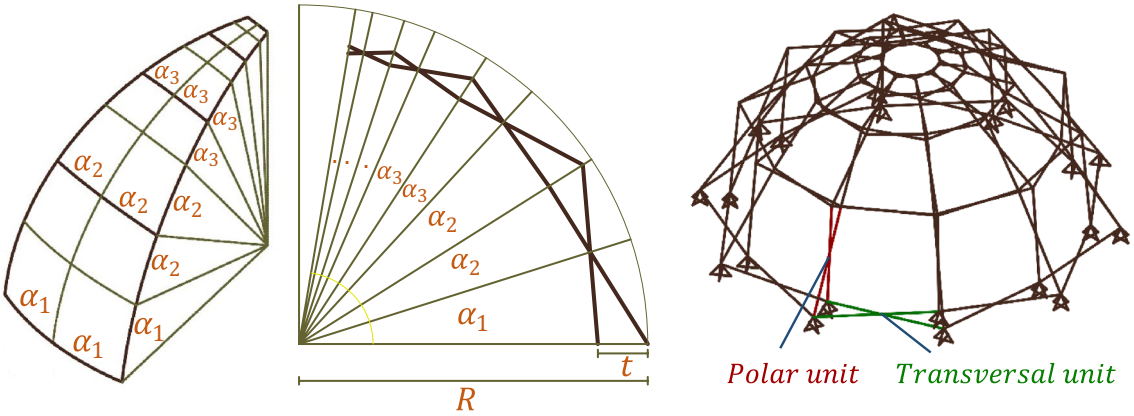

Fig. 6 A spherical foldable structure

$$
\begin{cases}
m_k = \dfrac{1/\mathrm{fit}(k)}{1\Big/\sum_{i=1}^{n}\frac{1}{\mathrm{fit}(i)}}, \quad k = 1, 2, \ldots, n \\
v_i = 0, \quad i = 1, 2, \ldots, \dfrac{n}{2} \\
v_i = x_{1-n/2} - x_i, \quad i = \dfrac{n}{2}+1, \ \dfrac{n}{2}+2, \ \ldots, \ n \\
v_i' = \dfrac{\left(m_{i+\frac{n}{2}} + \varepsilon m_{i+\frac{n}{2}}\right) \times v_{i+\frac{n}{2}}}{m_i + m_{i+\frac{n}{2}}}, \quad i = 1, 2, \ldots, \dfrac{n}{2} \\
v_i' = \dfrac{(m_i - \varepsilon m_{i-\frac{n}{2}}) \times v_i}{m_i + m_{i-\frac{n}{2}}}, \quad i = \dfrac{n}{2}+1, \dfrac{n}{2}+2, \ldots, n \\
\varepsilon = 1 - \dfrac{\mathrm{iter}}{\mathrm{iter}_{\max}} \\
x_i^{\mathrm{new}} = x_i \times \mathrm{rand}.v_i', \quad i = 1, 2, \ldots, \dfrac{n}{2} \\
x_i^{\mathrm{new}} = x_{i-\frac{n}{2}} \times \mathrm{rand}.v_i', \quad i = \dfrac{n}{2}+1, \dfrac{n}{2}+2, \ldots, n.
\end{cases}
\tag{9}
$$

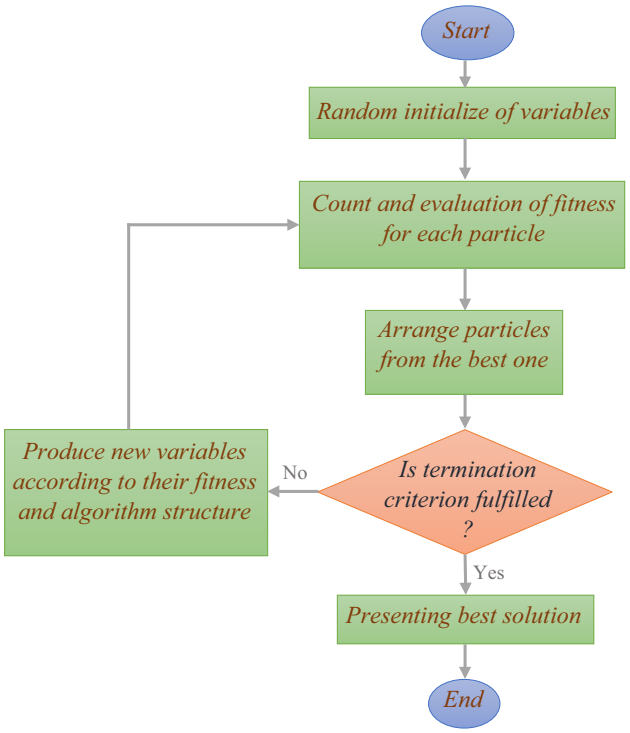

Fig. 7 Flowchart of the optimization algorithm

Colliding bodies optimization works based on the collision of particles (9). Each particle has its own variables and weight (m_k). The weights of the particles correspond to their cost; Particles with less cost are heavier. In each iteration, particles are divided into two groups (Fig. 8) stationary and moving. Moving particles collide with stationary ones with primary velocity (v_i). After the collision, each particle updates its velocity (v_i'). According to Eq. (9), the updated velocity of heavier particles is less than lightweight particles; It causes the algorithm to converge to a better particle which corresponds to less cost.

If there is more than one objective in the optimization issue, multi-objective meta-heuristic algorithms should be used. These algorithms are established on the basic meta-heuristic algorithm, but the solution space is divided by the number of objectives. Multi-objective optimization algorithms try to find an area of solutions that minimize all objective functions simultaneously. Multi-objective, genetic algorithm, NSGA-II, is presented in Deb et al. [19]. In this paper, a multi-objective version of the CBO algorithm (MOCBO) [20] is utilized using the NSGA-II method.

In multi-objective algorithms, particles take place in search space. They are divided into different groups by their front number (Fig. 9). The first front contains particles that do not concur with other best front. By excluding particles of the first front from solution space, the particles that do not concur would be in the next front. It continues until all particles take place in different fronts. A particle can concur with others if it has better cost at least in one objective than them. In each front, particles are graded for their distance from others. Particles that have more crowding distance will have higher value. This helps the algorithm to cover all parts of the solution area.

Multi-objective colliding body formulation is exactly like the standard CBO (9), but the difference is in the weight of the particles. In the MOCBO, the weights of the particles are assigned by Eq. (10).

$$
m_k = \frac{\mathrm{nf} + \mathrm{cr}_k + 1 - \mathrm{pf}_k}{\mathrm{nf}}, \quad k = 1, 2, \ldots, n, \tag{10}
$$

$\mathrm{cr}_k = 1$ For end particles of front,

$$
\mathrm{cr}_k = \sum_{i=1}^{g} \frac{|\cos t_{k+1}^i - \cos t_{k-1}^i|}{|\cos t_{\mathrm{end}}^i - \cos t_1^i|} \quad \text{For middle particles of front.}
$$

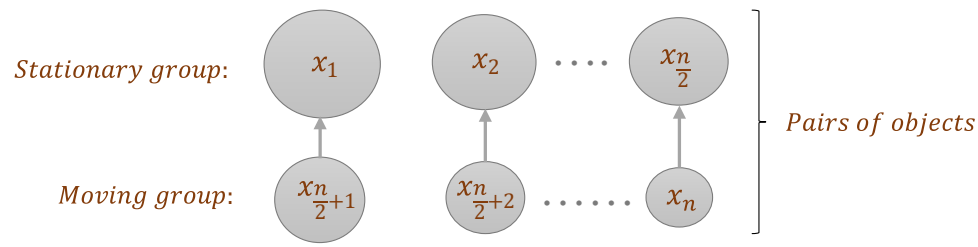

Fig. 8 Pairing of the particles of the colliding bodies optimization [9]

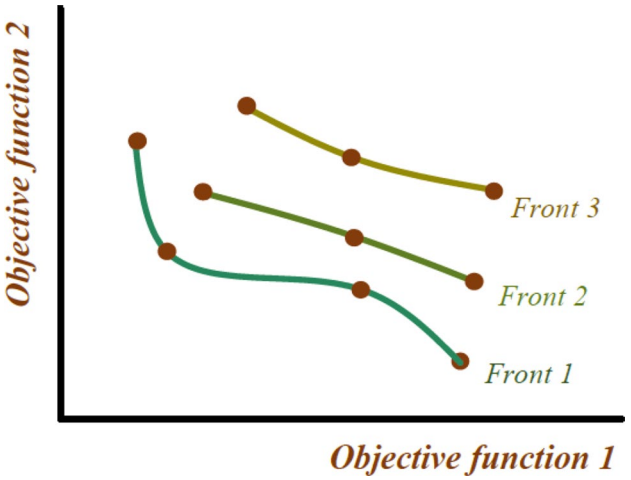

Fig. 9 Objective function space

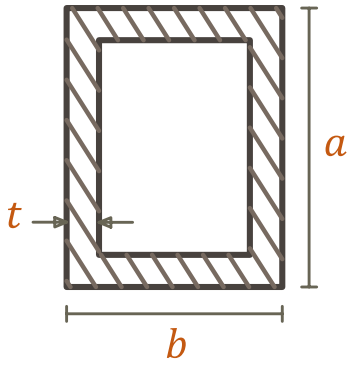

Fig. 10 Element cross section

m_k: weight of the particle, nf: number of fronts, pf: front number of particle, cr: crowding distance of particles, g: number of the objective functions.

Another feature of the MOCBO algorithm is that in each iteration, the best front particles combine to the next generation to save the best positions, and then they are sorted according to their weight to achieve the best population; this part is similar to the ECBO [21].

5 Numerical studies

In this paper, one barrel vault and one spherical dome are optimized by the NSGA-II and MOCBO algorithms. The objective functions of the optimization consist of the weight (11) and volume (12) of structures. The material used for elements is aluminum 6061-T4 ($E = 70$ GPa, $f_y = 110$ MPa, $\rho = 2727$ kg/m^3, $\upsilon = 0.33$). The cross sections of elements are rectangular tubes (Fig. 10):

$$w = N_j \times w_j + \sum_{i=1}^{N} \rho \times A_i \times L_i, \tag{11}$$

$$v = \sum_{i=1}^{N} (a \times b)_i \times L_i, \tag{12}$$

N: number of elements, A: section-sectional area, L: length of the element, N_j: number of joints, w_j: weight of the joints.

Optimization variables are presented in Table 1. The number of scissor units is the number of units in one arch in a barrel vault, and it is the number of units in the base semicircle of the spherical dome. Optimization constraints are maximum displacements, allowable stress and control of the element buckling.

- Permissible displacement is $R/50$, and R is the radius of structure.
- Allowable stress is 110 MPa according to the material, 6061-T4.
- Buckling of elements is checked by Eurocode 9.

Wind and snow loads are imposed on the structures according to Eurocode, as shown in Figs. 11 and 12. The basic velocity for wind load and the height of sea level are considered as 21 m/s and 26 m, respectively The weight of each joint is 0.5 kg. A uniform PVC membrane 0.7 kg/m^2 is considered on the structures. All the loads are equalized to external nodes of structures. Equation (13) is used for load combination in this paper. This load combination has more effect on these structures:

$$1.5 \times w + 0.75 \times s + 1.35 \times G. \tag{13}$$

In both optimization algorithms, the numbers of iterations and populations are taken as to 150 and 50, respectively.

Table 1 Optimization variables and their lower and upper limits

Optimization variable	Lower limit	Upper limit
Number of scissor units	5	10
Thickness of arch	15 cm	50 cm
Height of polar elements	12 mm	120 mm
Width of polar elements	12 mm	120 mm
Thickness of polar elements	1.2 mm	6.3 mm
Height of translational elements	12 mm	120 mm
Width of translational elements	12 mm	120 mm
Thickness of translational elements	1.2 mm	6.3 mm

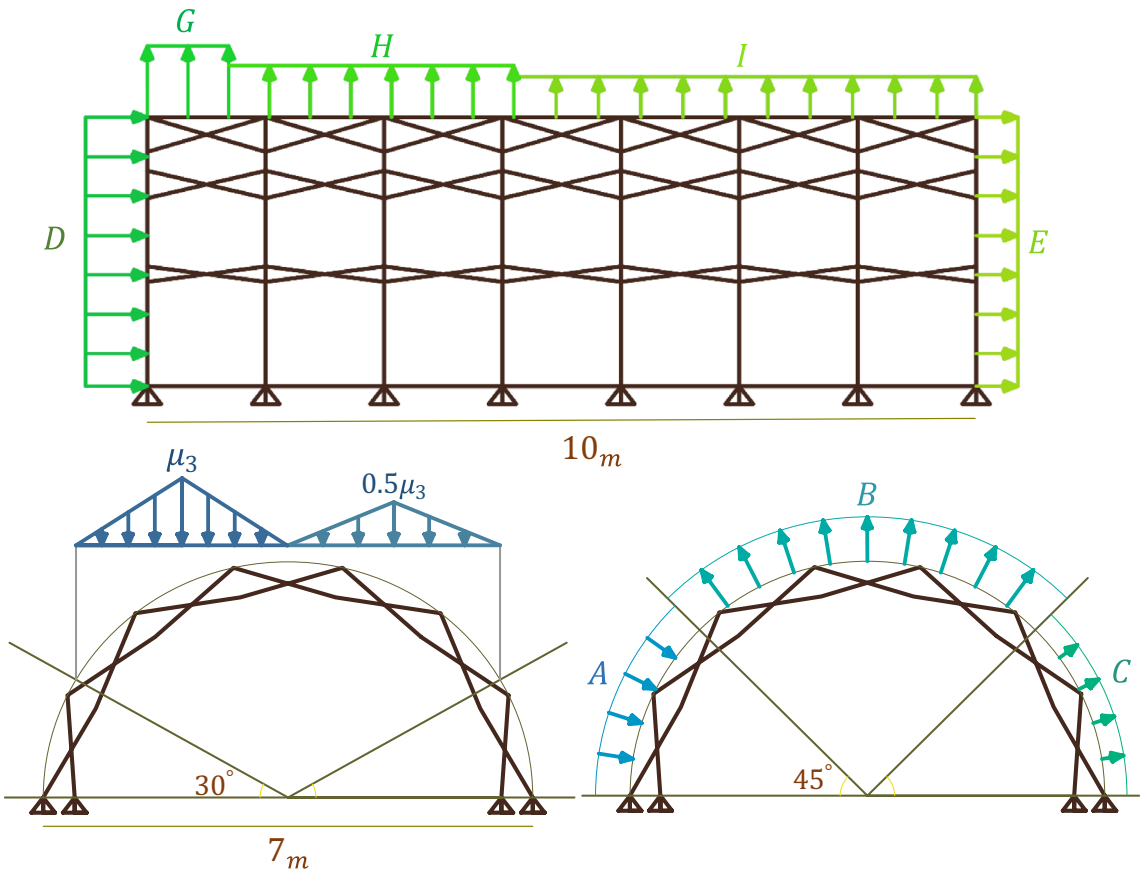

Fig. 11 Lateral wind load, drift snow, and longitude wind load to barrel vault

Fig. 12 Imposed snow and wind load on spherical dome

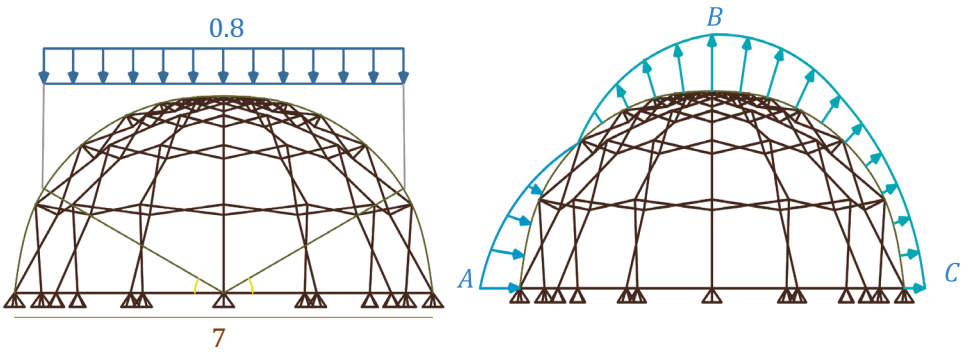

5.1 Optimization of barrel vault

The first part of this study consists of an optimal design of a barrel vault foldable structure hinged to the ground by four supports in each arch. Wind load is imposed on the structure in two directions (Fig. 11). The structure is analyzed by combination of lateral wind load with other load cases, and it is also analyzed by combination of longitudinal wind load with other load cases. Radius and length of the barrel vault are constant and equal to 3.45 and 10 m. The number of arches in the length of the structure depends on the number of units in the arch to keep the structure's length fixed. Some of the results obtained by the MOCBO and NSGA-II are presented in Tables 2 and 3, respectively. Figure 13 shows the range of the results in search space and the achieved optimal solution of the objectives by both algorithms.

5.2 Optimization of spherical dome

The other studied structure is a spherical dome foldable structure. All basic nodes of the structure are connected to the ground. Figure 12 shows the imposed wind and snow loads on the structure. Figure 14 shows the different particles in search space and the obtained minimum objectives in some different iteration. Variables parameters of selective particles from MOCBO and NSGA-II are presented in Tables 4 and 5.

6 Conclusions

This research is divided into two parts. In the first part, for the first time it presents a finite element method for the analysis of scissor-link foldable structure. This method results in a real analysis of scissor-link foldable structures by considering all degrees of freedom of the structure. Another feature of this method is avoiding complicated simulation using the existing softwares. In addition, it consumes less time for analysis of foldable structures in comparison to the analysis by existing softwares. Reduction of time consumption is important especially in optimization because of the large number of analyses being needed.

The second part is allocated to the optimal design of these structures. Two multi-objective meta-heuristic algorithms are used. Both algorithms present a wide range of designs that balance between the weight and volume of the structures. The presented designs by these algorithms satisfy all the constraints. The repetitive analysis shows that the proposed MOCBO algorithm covers a bigger range

Table 2 Variables obtained by the MOCBO algorithm for the barrel vault

Number of units	Height of polar elements	Width of polar elements	Thickness of polar elements	Height of translational elements	Width of translational elements	Thickness of translational elements	Thickness of arch	Weight of structure	Volume of structure
5	34	90	6.4	12	20	3.5	50	553.73	0.3862
5	40	99	4.1	12	20	3.0	50	426.63	0.4235
5	53	108	2.8	13	18	3.0	43	356.08	0.4771
5	72	111	2.1	15	21	1.9	40	305.86	0.5452
5	95	115	1.6	14	21	1.9	41	273.52	0.6095
5	120	120	1.2	12	30	1.7	44	247.50	0.7054

Table 3 Variables obtained by the NSGA-II algorithm for the barrel vault

Number of units	Height of polar elements	Width of polar elements	Thickness of polar elements	Height of translational elements	Width of translational elements	Thickness of translational elements	Thickness of arch	Weight of structure	Volume of structure
5	59	83	3.9	12	42	3.2	47	469.52	0.4861
5	57	86	3.6	12	42	2.7	50	430.63	0.4879
5	61	94	3.1	12	35	1.4	50	363.89	0.5003
5	69	96	2.6	12	38	1.3	50	332.17	0.5325
5	83	96	2.2	12	40	1.2	50	309.13	0.5721
5	92	97	1.8	35	42	1.2	50	295.09	0.6588

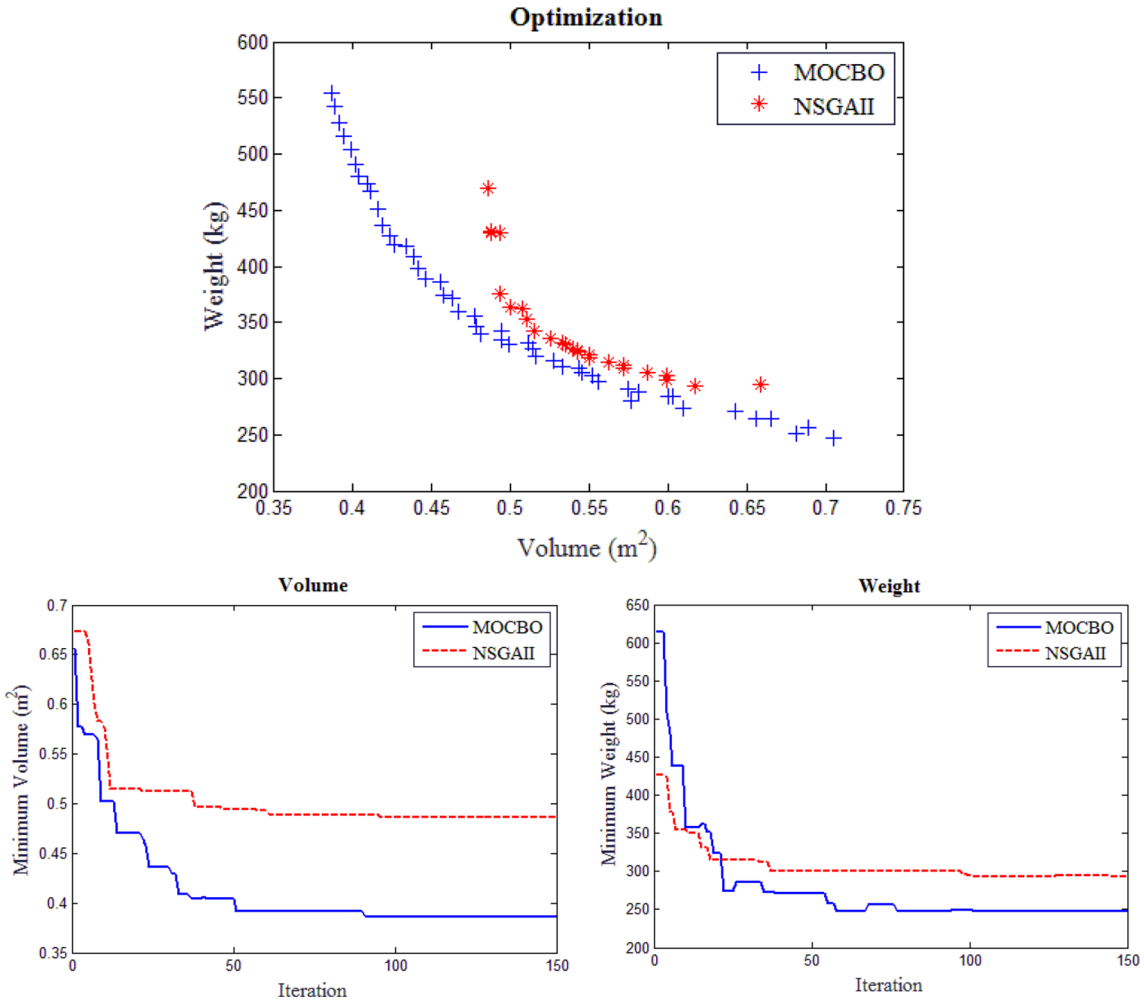

Fig. 13 Optimization results of the barrel vault

of search space and it is more powerful to get minimum objectives.

The covered area by the considered barrel vault structure is 70 m^2 and the minimum weight obtained by MOCBO algorithm is 247 kg. Also, covered area by the considered dome structure is 38 m^2 and its minimum weight is 103 kg. A comparison of these values shows that the optimized structures have acceptable weights and can be considered as suitable structures.

Finally, foldable structures are divided into two categories: compatible and incompatible. Compatible foldable structures show stress release during the folding process, but incompatible one has nonlinear behavior during the folding process [22]. The studied structures in this paper are compatible and do not need nonlinear analysis.

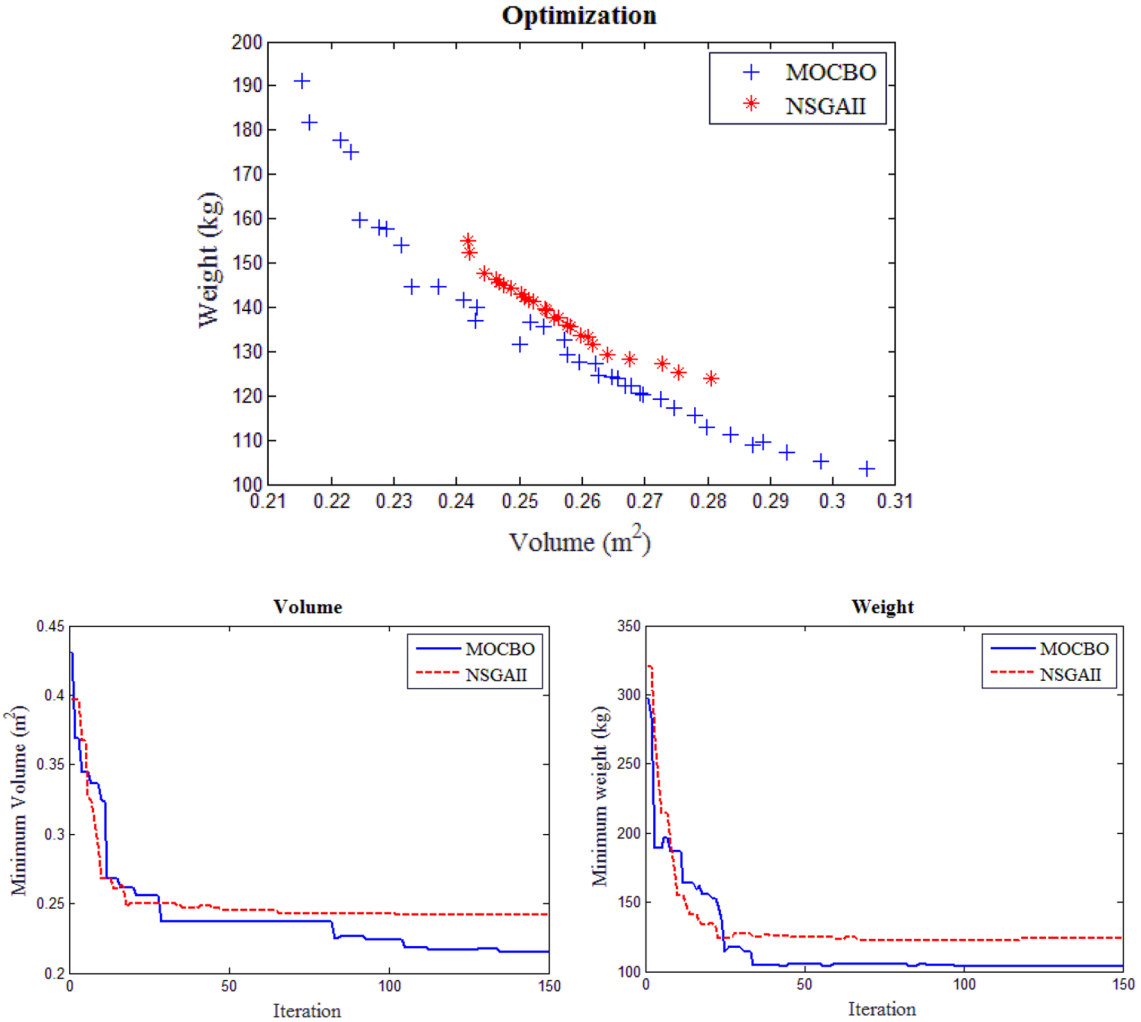

Fig. 14 Optimization results of the spherical dome

Table 4 Variables obtained by the MOCBO algorithm for the spherical dome

Number of units	Height of polar elements	Width of polar elements	Thickness of polar elements	Height of translational elements	Width of translational elements	Thickness of translational elements	Thickness of arch	Weight of structure	Volume of structure
5	20	38	4.8	12	35	2.5	38	191.17	0.2153
5	23	38	3.9	12	36	2.3	39	175.05	0.2230
5	21	42	2.9	12	38	2.2	40	154.10	0.2311
5	26	40	2.6	12	47	1.3	42	132.56	0.2571
5	28	47	1.8	12	49	1.2	44	115.47	0.2778
5	32	58	1.2	12	49	1.2	43	103.67	0.3054

Table 5 Variables obtained by the NSGA-II algorithm for the spherical dome

Number of units	Height of polar elements	Width of polar elements	Thickness of polar elements	Height of translational elements	Width of translational elements	Thickness of translational elements	Thickness of arch	Weight of structure	Volume of structure
5	20	43	2.8	29	26	2.1	46	154.99	0.2418
5	21	45	2.4	28	27	2.0	44	145.14	0.2475
5	21	45	2.4	28	30	1.7	45	139.16	0.2543
5	22	47	2.1	28	30	1.7	45	133.69	0.2598
5	25	51	1.7	28	30	1.7	44	127.35	0.2727
5	27	51	1.6	28	32	1.6	47	123.99	0.2805

References

1. Mira LA, Thrall AP, De Temmerman N (2014) Deployable scissor arch for transitional shelters. Autom Construct 43:123–131. https://doi.org/10.1016/j.autcon.2014.03.014
2. Shan W (1992) Computer analysis of foldable structures. Comput Struct 42(6):903–912. https://doi.org/10.1016/0045-7949(92)90102-6
3. Kaveh A, Davaran A (1996) Analysis of pantograph foldable structures. Comput Struct 59(1):131–140. https://doi.org/10.1016/0045-7949(95)00231-6
4. Escrig F (1985) Expandable space structures. Int J Space Struct 1(2):79–91. https://doi.org/10.1177/026635118500100203
5. Hernandez C, Transformables E, Estran I (1988) Geometry of expanable structures. In: Tecnologia y Construction, vol. 4, pp 103–118 (Caracas)
6. Escrig F, Valcarcel JP (1993) Geometry of expandable space structures. Int J Space Struct 8(1–2):71–84. https://doi.org/10.1177/0266351193008001-208
7. Escrig F, Sanchez J, Valcarcel JP (1996) Two way deployable spherical grids. Int J Space Struct 11(1–2):257–274. https://doi.org/10.1177/026635119601-231
8. Escrig F, Sanchez J (2006) New designs and geometries of deployable scissor structures. In: Proceedings of Adaptables2006, TU/e, international conference on adaptable building structures Eindhoven (The Netherlands), pp 5–18
9. Kaveh A, Mahdavi VR (2014) Colliding bodies optimization: a novel meta-heuristic method. Comput Struct 139:18–27. https://doi.org/10.1016/j.compstruc.2014.04.005
10. Kaveh A, Ilchi Ghazaan M (2017) A new meta-heuristic algorithm: vibrating particles system. Scientia Iranica Trans A Civ Eng 24(2):551–566
11. Kaveh A, Dadras A (2017) A novel meta-heuristic optimization algorithm: thermal exchange optimization. Adv Eng Softw 110:69–84. https://doi.org/10.1016/j.advengsoft.2017.03.014
12. Kaveh A, Jafarvand A, Barkhordari MA (1999) Optimal design of pantograph foldable structures. Int J Space Struct 14(4):295–302. https://doi.org/10.1260/0266351991494911
13. Kaveh A, Shojaee S (2004) Optimal design of scissor-link foldable structures using genetic algorithms. Paper 94 from CCP: 80. ISBN:0-948749-98-9
14. Kaveh A, Shojaee S (2007) Optimal design of scissor-link foldable structures using ant colony optimization algorithm. Comput Aided Civ Infrastruct Eng 22(1):56–64. https://doi.org/10.1111/j.1467-8667.2006.00470.x
15. Alegria Mira L, Thrall AP, De Temmerman N (2016) The universal scissor component: optimization of a reconfigurable component for deployable scissor structures. Eng Optim 48(2):317–333. https://doi.org/10.1080/0305215X.2015.1011151
16. Thrall AP, Zhu M, Guest JK, Paya-Zaforteza I, Adriaenssens S (2012) Structural optimization of deploying structures composed of linkages. J Comput Civ Eng 28(3):04014010. https://doi.org/10.1061/(ASCE)CP.1943-5487.0000272
17. Koumar A, Tysmans T, De Temmerman N, Coelho RF, Mira LA (2014) Multi-criteria optimization of a barrel vault structure for emergency relief. In: Proceedings of the symposium: shells, membranes and spatial structures: footprints (IASS-SLTE'14)
18. Koumar A, Tysmans T, Filomeno Coelho R, De Temmerman N (2017) An automated structural optimisation methodology for scissor structures using a genetic algorithm. Appl Comput Intell Soft Comput. https://doi.org/10.1155/2017/6843574 2017.
19. Deb K, Pratap A, Agarwal S, Meyarivan TAMT. (2002) A fast and elitist multiobjective genetic algorithm: NSGA-II. IEEE Trans Evol Comput 6(2):182–197. https://doi.org/10.1109/4235.996017
20. Panda A, Pani S (2016) Multi-objective colliding bodies optimization. In: Proceedings of fifth international conference on soft computing for problem solving. Springer, Singapore, pp 651–664. https://doi.org/10.1007/978-981-10-0448-3_54
21. Kaveh A, Ilchi Ghazaan M (2014) Computer codes for colliding bodies optimization and its enhanced version. Int J Optim Civ Eng 4(3):321–332
22. Gantes CJ, Connor JJ, Logcher RD, Rosenfeld Y (1989) Structural analysis and design of deployable structures. Comput Struct 32(3–4):661–669. https://doi.org/10.1016/0045-7949 (89)90354-4